



Aalborg Universitet

AALBORG UNIVERSITY
DENMARK

Power Sharing in Three-level NPC Inverter based Three-Phase Four-Wire Islanding Microgrids with Unbalanced Loads

Sharma, Binod; Pankaj, Prabhat K.; Terriche, Yacine; Saim, Abdelhakim; Shrestha, Ashish; Su, Chun Lien; Guerrero, Josep M.

Published in:
IEEE Access

DOI (link to publication from Publisher):
[10.1109/ACCESS.2023.3250219](https://doi.org/10.1109/ACCESS.2023.3250219)

Creative Commons License
CC BY-NC-ND 4.0

Publication date:
2023

Document Version
Publisher's PDF, also known as Version of record

[Link to publication from Aalborg University](#)

Citation for published version (APA):
Sharma, B., Pankaj, P. K., Terriche, Y., Saim, A., Shrestha, A., Su, C. L., & Guerrero, J. M. (2023). Power Sharing in Three-level NPC Inverter based Three-Phase Four-Wire Islanding Microgrids with Unbalanced Loads. *IEEE Access*, 11, 20725-20740. <https://doi.org/10.1109/ACCESS.2023.3250219>

General rights

Copyright and moral rights for the publications made accessible in the public portal are retained by the authors and/or other copyright owners and it is a condition of accessing publications that users recognise and abide by the legal requirements associated with these rights.

- Users may download and print one copy of any publication from the public portal for the purpose of private study or research.
- You may not further distribute the material or use it for any profit-making activity or commercial gain
- You may freely distribute the URL identifying the publication in the public portal -

Take down policy

If you believe that this document breaches copyright please contact us at vbn@aub.aau.dk providing details, and we will remove access to the work immediately and investigate your claim.

RESEARCH ARTICLE

Power Sharing in Three-Level NPC Inverter Based Three-Phase Four-Wire Islanding Microgrids With Unbalanced Loads

BINOD SHARMA¹, **PRABHAT KUMAR PANKAJ**², **YACINE TERRICHE**³,
ABDELHAKIM SAIM⁴, **ASHISH SHRESTHA**⁵, (Member, IEEE),
CHUN-LIEN SU⁶, (Senior Member, IEEE), **AND JOSEP M. GUERRERO**³, (Fellow, IEEE)

¹Pokhara Grid Section, Nepal Electricity Authority, Pokhara 33700, Nepal

²Load Dispatch Center, Nepal Electricity Authority, Kathmandu 44600, Nepal

³AAU Energy, Aalborg University, 9220 Aalborg, Denmark

⁴IREENA Laboratory, University of Nantes, 44600 Saint-Nazaire, France

⁵Department of Electrical Engineering, Information Technology and Cybernetics, University of South-Eastern Norway, 3918 Porsgrunn, Norway

⁶Department of Electrical Engineering, National Kaohsiung University of Science and Technology, Kaohsiung City 807618, Taiwan

Corresponding author: Chun-Lien Su (cls@nkust.edu.tw)

The work of Chun-Lien Su was supported by the National Science and Technology Council of Taiwan under Grant MOST 110-2221-E-992-044-MY3.

ABSTRACT The droop-based control schemes are widely used for power-sharing and control of the isolated microgrids. The conventional droop control scheme with inner current and voltage controllers can work effectively under ideal voltage. However, the existence of unbalance tends its performance to worsen. This paper aims to propose an enhanced droop control method to improve the power-sharing, and maintain the distributed generators' (DGs) terminal voltages and the system frequency under the balanced as well as unbalanced loads. The enhancements of the proposed control scheme include the droop controller, inner current and voltage controller, and virtual impedance loop. The proposed virtual impedance deals with the accurate sharing of powers in the case of unequal line impedance and the control of zero sequence current. Moreover, to enable the proposed control to compensate for the unbalance, three-level neutral point clamped (NPC) inverters are used to form a three-phase four-wire microgrid. With this control scheme, the voltage unbalance factors (VUFs) of the DGs' terminal voltages are reduced from 4% to less than 1%, negative sequence reactive powers, which are also an indication of unbalance, have been reduced significantly, and the system frequency is maintained within the standard permissible limit of 2.5%. Furthermore, a local load controller is also proposed to control the reactive loading of the DGs when they have local loads supplied from their terminals. The investigations have been carried out under simulation as well as lab-based environments to validate the efficacy of the proposed control method.

INDEX TERMS Droop control, local load controller, power-sharing, three-phase four-wire power systems, unbalanced loads, virtual impedance.

I. INTRODUCTION

To utilize the small-scale local renewable energy sources (RES), the concept of distributed generation (DG) has been developed. Multiple DGs can be connected in parallel to increase the system generation capacity, system reliability,

The associate editor coordinating the review of this manuscript and approving it for publication was Suman Maiti.

security, and so on; called microgrid concept [1]. The concept of microgrids was developed to achieve more power supply reliability by utilizing the local renewable resources [2], [3]. Basically, microgrid operates in two modes: (a) isolated, and (b) grid connected [4]. The operation of microgrids in isolated mode can create more challenges that can affect the system voltage, frequency, and DGs power-sharing [5]. With the development of grid-forming inverters, it has been possible to

operate inverters-based microgrids in an isolated mode. However, inverters-based microgrids are comparatively sensitive over conventional synchronous generators-based system, and affected by small disturbances, interaction among inverters, power-sharing etc [6].

The active power/ frequency (P/f) and reactive power/ voltage (Q/V) droop control with inner current and voltage controllers is a very popular control scheme to operate the microgrids in an isolated mode. The droop control method is widely applied in isolated microgrids as a distributed control mechanism due to its simplicity, dependency on the local parameters, and flexibility. However, the conventional droop control still struggles from inherent limitations such as the trade-off between voltage regulation and load sharing, affected by line impedance mismatch, poor transient performance, poor unbalanced and harmonic power-sharing [7]. The concept of virtual impedance is extensively used to solve the problems created by line impedance mismatch [8], [9], [10]. A resistive virtual impedance in droop control improves dynamic response and non-linear power-sharing in addition to the impedance mismatch [11]. An adaptive transient droop function is combined with conventional droop control to improve transient response and power-sharing stability [12]. The droop-based control scheme is upgraded to share the powers accurately without compromising the voltage regulation by adding an external secondary controller to restore the inherent deviations created in voltage and frequency due to the conventional droop control [13].

The performance of conventional droop control isn't satisfactory under unbalanced load conditions. To date, many attempts from different approaches have been made to deal with the droop-controlled microgrid feeding the unbalanced loads. Active power filters and FACTS devices can be a very effective solution to deal with voltage/current unbalance. However, their high cost limits their application, particularly for small-scale capacity microgrids where they need to inject large power in case of a severe unbalance [14], [15]. Another approach that has been widely proposed in papers to deal with unbalance is to damp or compensate for the unbalance components. The negative sequence components of reactive power can be taken as the indication of unbalance in three-phase three-wire systems [16]. Hence, many methods have been proposed to reduce the effect of unbalance by controlling the negative sequence components such as the reactive power-impedance (Q-Z*) droop control technique [17] and virtual negative sequence impedance loop-based controller [18]. Thus, virtual impedance, which was initially used for the purpose of DG output impedance matching and power decoupling, is also being used for the compensation of unbalance components. The only difficulty associated with virtual impedance is the prediction of its numerical values, which has been solved by making it adaptive [19]. Though this concept provides satisfactory performance under a three-phase three-wire configuration, it can't give the desired performance in a

three-phase four-wire microgrid because of the existence of zero sequence components in the latter configuration. In real applications, the low-voltage three-phase microgrids always need four wires to supply the single-phase loads, provide a path for the unbalanced current, and facilitate earth fault protection. Hence, the zero-sequence component appears in the neutral and needs to be controlled [20]. Recently, a few papers have considered four-wire microgrid configuration in their study and proposed a control strategy based on the virtual negative and zero sequence impedance [21]. However, this approach becomes really complicated because of the addition of an extra zero sequence impedance loop and sequence component separation requirement. Another interesting concept proposed to improve unbalanced power-sharing is to use fundamental positive sequence (FPS) components in the droop controller so that the influence of unbalanced sequence components in generating the voltage reference and thus in power-sharing avoided [22], [23], [24]. This paper proposed a control scheme for an islanded microgrid operating with an unbalanced load by combining a virtual impedance approach and an FPS-based droop control concept, so that a simple virtual impedance gives a satisfactory performance.

Generally, two strategies are used in unbalanced control methods, per phase control strategy and symmetrical components control strategy. The per-phase control strategy is used in the three-phase four-wire system so that each phase can be independently controlled [25]. There are three widely used inverter topologies to form a three-phase four-wire microgrid including Four limb inverter, Capacitor midpoint inverter, and three H-bridge inverter [25]. However, each topology has some limitations. The four limb inverters suffer from a few issues such as increased control and hardware requirement, and electromagnetic interference due to high-frequency operation of the neutral leg [26], [27]. The conventional two-level split capacitor inverters face high stress on the switches, low dc voltage utilization, and poor voltage sharing between the split capacitors [28]. The applications of H-bridge inverters are also limited due to their size and the need for a separate dc source for each phase [29], [30]. Under these circumstances, three-level NPC inverters could be an effective alternative for the formation of three-phase four-wire microgrid as they offer reduced stresses on the switches, proper voltage sharing across the switches due to the use of clamping diodes, and good voltage balancing of the split capacitors as unbalance current flows to neutral through the switches, not through the split capacitors [31], [32], [33]. To the best knowledge of the authors, the three-level NPC inverters haven't been used for the formation of the three-phase four-wire microgrid previously.

This paper presents an enhanced droop control scheme that improve the power-sharing of three-level neutral point clamped (NPC) inverters-based three-phase four-wire isolated microgrid under an unbalanced condition. The unbalanced condition is placed at the point of common coupling (PCC) and the local loads supplied from the DGs' terminals.

The proposed control scheme tries to compensate for the unbalance created by unbalanced loads and improves the effective sharing of powers. However, the harmonics-related issues due to non-linear loads aren't considered in this paper. Moreover, the performance of the proposed control scheme under load disturbances is observed considering step load changes at the DGs' terminals and PCC. The three-level NPC inverters are chosen for the development of the three-phase four-wire microgrids over two-level inverters as they do not require an extra limb for the neutral and have reduced stresses on the switches on high power applications and low harmonic content in the outputs [34]. In the proposed technique, only FPS component powers are used in the droop controller to reduce the influence of unbalance components in the voltage reference. The zero sequence components are controlled and compensated by the proposed virtual impedance. The balanced voltage reference obtained from the droop controller is tracked with the help of proportional resonant (PR) controllers in all $\alpha\beta 0$ -axes. The use of PR controllers in all $\alpha\beta 0$ -axes in the voltage and current controllers help to diminish the effects of the neutral voltage shifting and zero sequence component to guarantee a balanced and stable voltage with optimum power-sharing under unbalanced loads. The concept of virtual impedance in all $\alpha\beta 0$ -axes is also incorporated to solve the problem created by the line impedance mismatch between DGs and PCC. The proposed virtual impedance incorporating impedance in the zero sequence component also helps to control the DG neutral currents under unbalanced power-sharing. Moreover, local loads in each DG terminal are considered to make the microgrid structure more realistic. A local load controller is proposed to improve the reactive power-sharing when the system has unequal local loads supplied from DG terminals. The test microgrid system considered in this paper is same as in [35]. The inner current and voltage controller are also modelled in the similar fashion. The main factor that differentiates this paper from [35] is the approach dealing with the unbalance. This paper proposed a control strategy with a different droop controller approach and virtual impedance to compensate for the unbalance whereas [35] is focused on sharing positive and negative components of powers effectively among the participating DGs.

In this paper, the authors aim to propose a droop-based control scheme for a NPC inverters-based isolated microgrid that guarantees the improvement in the power-sharing as well as the control efficacy. Though described in detail in further chapters, the main contributions of this paper are:

1. A control scheme for the three-level NPC inverters-based three-phase four-wire isolated microgrid is proposed, with which the DGs' terminal voltages are kept in balance with better VUFs even under unbalanced loads, so the microgrid stays stable. The operation of isolated microgrids under unbalanced loads is further improved by compensating the negative sequence reactive power.

2. The concept of a virtual impedance loop is improved to control the DGs' neutral currents under unbalanced load

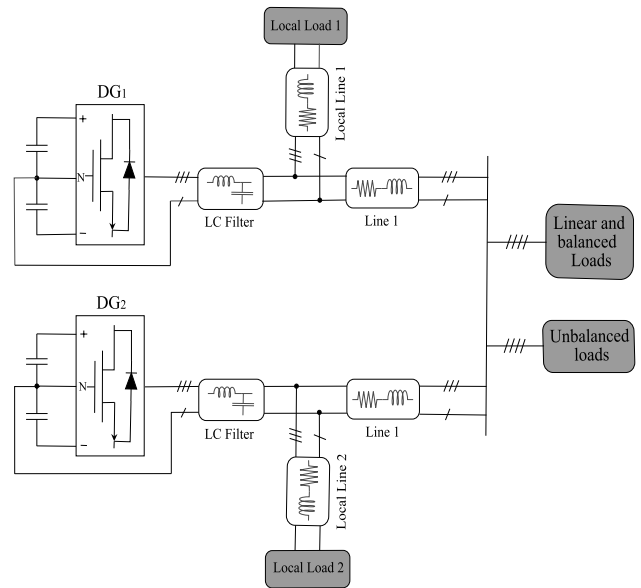


FIGURE 1. Test microgrid layout.

conditions. After the application of this concept, power-sharing is found to be improved.

3. To present a more realistic view of a microgrid, local loads supplied from DGs' terminals are also taken into consideration and a novel local load controller has been proposed to enhance the reactive power-sharing between the DGs.

4. The proposed scheme has been verified through experiments under simulation as well as a laboratory environment. Both experiments provide satisfactory results.

This paper first introduced the technical background, scientific activities, research gaps and motivation through literature reviews. Section II presents an overview of the adopted layouts of the microgrid and the components. The detailed power calculation is discussed in Section III. After that, the system modeling of each component found in a typical microgrid is presented in Section IV. The outcomes contained from the simulation as well as the experimental analysis are detailly presented in Section V. Finally, in Section VI, conclusions are drawn and presented based on the results and discussion.

II. MICROGRID SYSTEM UNDER STUDY

The layout of the test microgrid system taken in this paper is shown in Figure 1. It consists of two DGs connected to the PCC through certain line impedances. A three-level inverter with a fixed DC voltage source in its input and a low pass LC filter in its output is considered as a DG. Linear balanced and unbalanced loads are supplied from the PCC and their switching is managed by the circuit breakers. The local loads are supplied from each DG terminal through certain local line impedance.

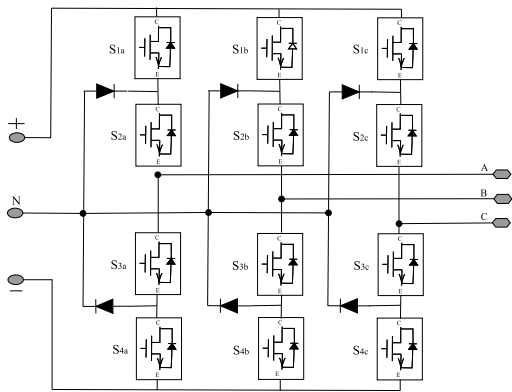


FIGURE 2. Three-level inverter.

A. THREE-LEVEL NPC INVERTER

In this paper, the three-phase four-wire microgrid is formed taking the clamped dc neutral of the three-level NPC inverter to the load terminal as the fourth wire neutral. The three-level NPC inverters used in this paper comprise insulated gate bipolar transistors (IGBT) and diodes as switches. The IGBTs have better switching characteristics than bipolar junction transistors (BJT) and more power handling capacity than metal oxide semiconductor field-effect transistors (MOS-FET). The three-level NPC inverters composed of IGBTs and diodes have many benefits over conventional two-level inverters such as reduced stress on switches, higher power rating capability, low harmonic content in output, ride-through capability, improved dynamic performance, higher efficiency, and lower cost [34], [36]. The schematic diagram of a three-level inverter is shown in Figure 2.

B. SELECTION OF LOW PASS LC FILTER

A common practice in filtering out the higher-order harmonics in inverter output is to use a low pass LC filter. The cut-off frequency of low pass filter (f_c) is a compromise between the attenuation effect and control bandwidth. The attenuation effect can be increased by decreasing the cut-off frequency, but a small cut-off frequency limits the control bandwidth. Increased control bandwidth is required for the inverter system [37]. Generally, the cut-off frequency is kept between $1/10^{\text{th}}$ of switching frequency and ten times the fundamental frequency, and the output voltage total harmonics distortion (THD) is kept less than 5%. The inductance of the series inductor filter (L_f) is selected such that the voltage drop across it remains within 3% of the inverter output voltage [38]. The capacitance of the shunt capacitor filter (C_f) is calculated from the cut-off frequency. Thus from above discussion, the cut-off frequency is obtained using equation 1.

$$10f_0 < f_c < (1/10)f_{sw} \tag{1}$$

and

$$I_{I_{max}} \times (2\pi fL) < 0.03V_{inv}. \tag{2}$$

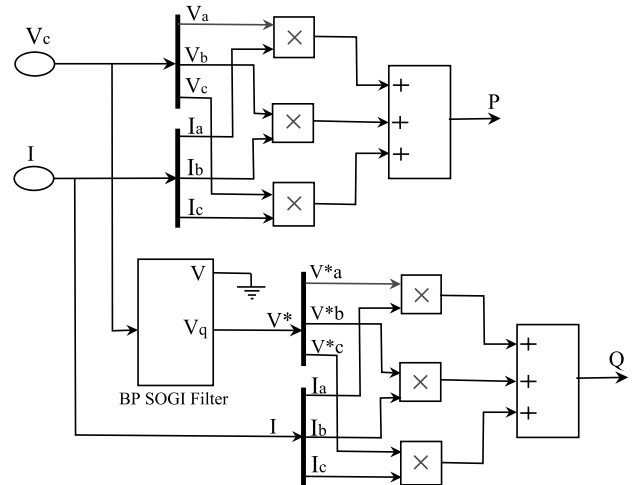


FIGURE 3. Power calculation.

where $I_{I_{max}}$ is the maximum RMS value of the load current and f is the frequency of the output voltage, V_{inv} .

Taking the value of switching frequency $f_{sw} = 18000\text{HZ}$, cut-off frequency $f_c = 750\text{HZ}$, inverter output phase voltage $V_{inv} = 230\text{V}$, and rearranging the equation (2). The filter inductor is calculated using equation 3.

$$L < (0.03 V_{inv}) / (I_{I_{max}} \times (2\pi f)) \tag{3}$$

Taking the value of filter inductor $L = 1.46\text{mH}$ for $I_{I_{max}} = 15\text{A}$, the filter capacitance can be calculated using 4.

$$C = 1 / ((2\pi f_c)^2 L) \tag{4}$$

Thus, values of filter inductor and capacitor used are $C = 30.8\mu\text{F}$, for $f_c = 750\text{Hz}$ and $L = 1.46\text{mH}$.

III. POWER CALCULATIONS

A. POWER CALCULATION IN ABC-REFERENCE FRAME

The instantaneous active and reactive powers shared by each DG can be calculated from the voltage of output capacitor (V_c), and DG current (I_l) using equations 5 & 6 respectively.

$$P_i = V_c \times I_l \tag{5}$$

$$Q_i = (jV_c) \times I_l \tag{6}$$

The per-phase active power is the product of the phase voltage and current. The reactive power is calculated by introducing a 90-degree phase delay in the voltage of the output capacitor and multiplying it with the DG current [39]. In this paper, the phase delay of 90-degree in the voltage of the output capacitor in reactive power calculation is achieved with the help of the second-order general integrator (SOGI). A SOGI has two outputs, one in phase with the input and the other in quadrature (90-degree lag) with the input [40]. The block diagram of the three-phase power calculation used in this paper for balanced as well as unbalanced load is shown in Figure 3.

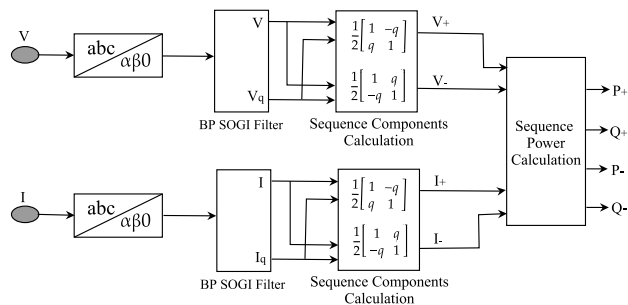


FIGURE 4. Sequence power calculation.

B. SEQUENCE POWER CALCULATION IN $\alpha\beta 0$ -REFERENCE FRAME

A balanced system has only positive sequence components of current and voltage. An unbalanced current or voltage can be decomposed into three balanced components as positive, negative, and zero sequence components. The sequence components of active and reactive power in $\alpha\beta 0$ -reference frame are calculated from the respective sequence components of current and voltage [41]:

$$P_{B1} = V_{\alpha}I_{\alpha} + V_{\beta}I_{\beta} \tag{7}$$

$$Q_{B1} = V_{\beta}I_{\alpha} - V_{\alpha}I_{\beta} \tag{8}$$

The block diagram of the sequence power calculation used in this paper is shown in Figure 4. A SOGI-bandpass filter (BPF) based structure has been used to extract the positive and negative sequence components of the current and voltage in $\alpha\beta 0$ -reference frame. Then respective sequence powers are calculated in the stationary reference frame from the extracted sequence components of current and voltage.

IV. THE PROPOSED CONTROL STRATEGY

Figure 5 presents the overall schematic diagram of the proposed control scheme in this study. It is identical for both of the DGs except the concept of virtual impedance is incorporated only in the voltage controller of the DG having smaller line impedance. The capacitor voltage and DG current in the abc-reference frame are taken for the active and reactive power calculation. A SOGI-BPF based power calculation block is introduced for the positive and negative sequence power calculation. Only the positive sequence active and reactive powers are supplied to the droop controller. The P/F and Q/V droops give angle and magnitude respectively for the generation of reference voltage in the abc-reference frame. The generated voltage reference is transformed into $\alpha\beta 0$ -reference frame and supplied to the voltage controller. The voltage controller compares the actual line voltage with the reference generated and the error signal is passed through a PR controller. This latter tracks the reference voltage with a minimum steady-state error. Regarding the line impedance mismatch, the effect of the virtual impedance is also introduced in the voltage controller of the DG having lower line impedance by multiplying the line current with the value of

this virtual impedance. Thus obtained virtual voltage drop is subtracted from the voltage reference so that the line impedance of the DG having lower line impedance is virtually increased. Now the line impedances have the same effect on their controllers even they actually have different values.

For the case with local loads, a local load controller is introduced in this paper to compensate for the effect of unequal local loads on reactive power-sharing and enables the reactive power to be shared equally between both DGs even when the local loads connected in each DG terminal are unequal.

The virtual voltage drop, which appears across the controller due to the presence of local load is compensated by the local load controller. The output of the voltage controller is used as a reference for the inner current controller. This reference is tracked by the PR controllers in the current control loop. As this paper has considered unbalanced loads in the test microgrid, the voltage and current controllers based in $\alpha\beta$ - axes are modified adding a PR controller in the 0-axis of $\alpha\beta 0$ -reference frame to track the reference in the same way used in the other phases. It enables control of the unbalanced effect. These controllers work well with both balanced and unbalanced loads. The neutral voltage shifting effect due to the unbalanced load is compensated by the PR controller in 0-axis of $\alpha\beta 0$ -reference of the voltage control loop and the unbalanced current in the neutral is controlled using the PR controller in 0-axis of $\alpha\beta 0$ -reference of the inner current control loop. The voltage controller regulates the voltage and reduces the unbalance. Thus, it enabled the voltage source inverters (VSIs) based microgrid to operate in the isolated mode with unbalanced and local loads. Finally, the controlled signal is transformed back to abc reference and passed to the three-level pulse width modulation (PWM) to generate the gate pulses.

A. DROOP BASED CONTROL SYSTEM

Master-slaves control, instantaneous current sharing control, and voltage and frequency droop control are generally used for power-sharing and control of an isolated microgrid. Among them, the droop control method is simple and independent as it requires no communication links. The droop control technique is developed from the operation of an alternator (i.e. when there is a large demand for active power, the alternator speed increases resulting in drooping the frequency). Similarly, when the reactive load on the alternator is increased, its voltage droops slightly. This principle has been now generalized in controlling the inverters-based microgrid. From static power flow equations, for an inductive line, the flow of power from DG to PCC can be expressed as:

$$P = EV\sin(\phi_E - \phi_Y)/X \tag{9}$$

$$Q = (E^2 - EV\cos(\phi_E - \phi_Y))/X \tag{10}$$

where E and V are the magnitudes of the inverter output voltage and PCC voltage, X is the line reactance. Thus, voltage and frequency droop equations for a microgrid can

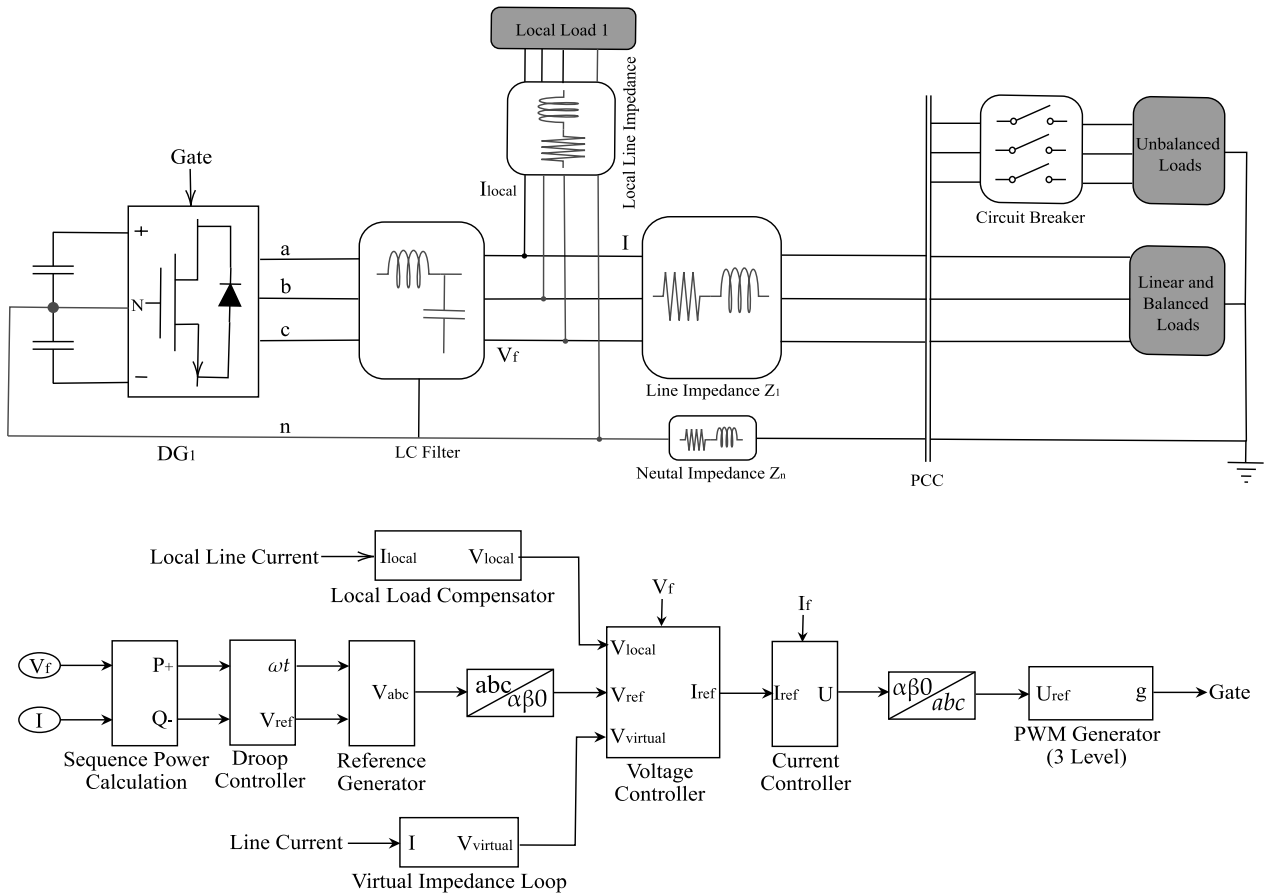


FIGURE 5. Overall controller block diagram.

be defined as:

$$\phi = \phi^* - mP \tag{11}$$

$$E = E^* - nQ \tag{12}$$

where $\phi^* = \int \omega^* dt$ and E^* are the references of the phase angle and magnitude of the voltage, m and n are the droop coefficients. Similarly, the droop equations can be derived for positive sequence powers as

$$\phi = \phi^* - (m_p P^+ + m_i \int P^+ dt) \tag{13}$$

$$E = E^* - nQ^+ \tag{14}$$

Equation (13) acts as a proportional-derivative controller for the frequency and improves the dynamic behavior of power sharing [14].

B. VIRTUAL IMPEDANCE CONCEPT

The virtual impedance concept in load sharing has been used for two purposes. One is for power decoupling and another is for impedance matching. The conventional droop equations are derived and the powers are decoupled considering the line to be inductive. While using conventional droop control for resistive lines, a large inductive impedance is virtually added

to the system so that the line could be assumed inductive. In this paper, the virtual impedance is used for impedance matching. When the lines connecting the DG to the PCC have different impedances, the voltage drop in the lines will be different. A circulating current flows from the DG with smaller line impedance to the DG with larger impedance due to the voltage difference. Then the power-sharing gets disturbed. As the reactive power-sharing is dependent on the voltage, it is mostly affected. To solve this problem, the impedance of the line with a smaller impedance is virtually increased to make it equal to the larger one. Virtual impedance required for DG_1 , Z_{1V} is calculated using equation 15.

$$Z_{1V} = S_2/S_1 \times (Z_2 - Z_1) \tag{15}$$

where S_2/S_1 is the ratio of the load sharing, and Z_1 and Z_2 are the impedances of the lines connecting the DG and PCC. In this paper, the virtual impedance concept for impedance matching as proposed in [8] is modified by adding an impedance in 0-axis of $\alpha\beta 0$ -reference frame to have equal neutral loading of DGs in the case of unbalanced power-sharing. The value of virtual impedance in 0-axis (Z_{0V}) is

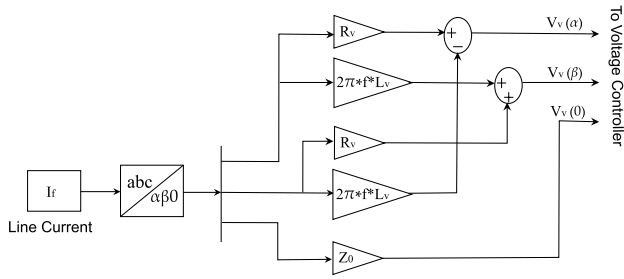


FIGURE 6. Virtual impedance implementation.

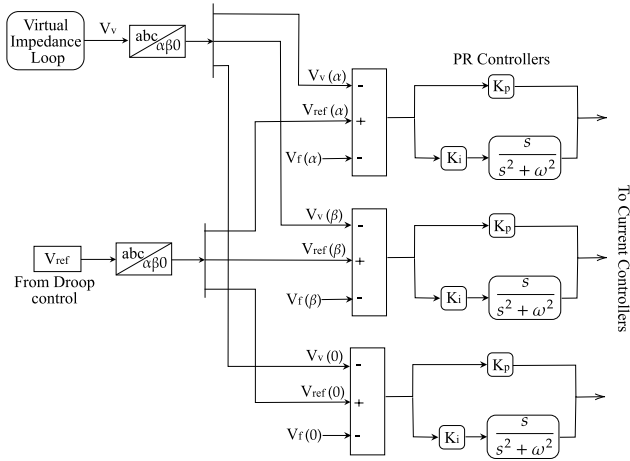


FIGURE 7. Voltage controller.

obtained using equation 16:

$$Z_{0V} = 3 \times \sqrt{(R_v^2 + \omega^2 L_v^2)} \quad (16)$$

The block diagram of the virtual impedance implementation is shown in Figure 6. It is named virtual as no physical impedance is used in the system. Only the voltage drop effect of the impedance is added in the controller just to equalize the unequal voltage drops due to unequal line impedance.

C. INNER CURRENT AND VOLTAGE CONTROLLERS

When unbalanced loads are connected to the system, the terminal voltages of the DGs also become unbalanced because of the unbalance voltage drop in the internal impedance of DG. An inverters-based system has a large unbalance voltage drop due to the presence of a large impedance low pass filter [42]. In this paper the test system contains unbalanced loads, so only the positive sequence active and reactive powers are used in the droop controller to produce a balanced reference signal. To facilitate an effective tracking of the reference, the voltage and current controllers used in [14] are modified by incorporating one additional PR controller in the 0-axis of $\alpha\beta 0$ -reference frame. The shifting of neutral voltage is regulated using a PR controller in the 0-axis of $\alpha\beta 0$ -reference in voltage controller as shown in Figure 7. The output of the voltage controller is tracked by an

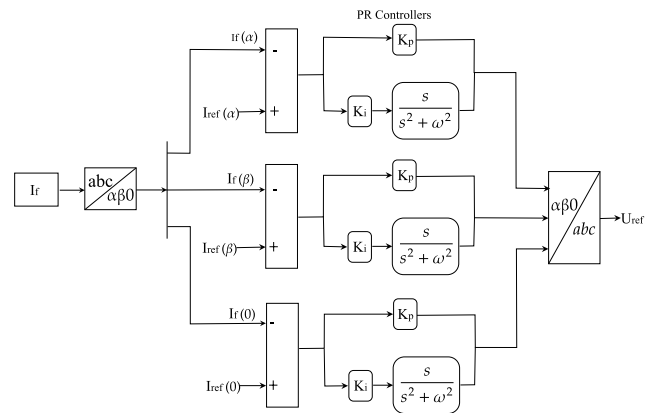


FIGURE 8. Current controller.

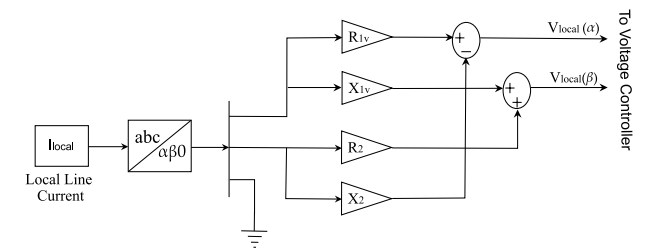


FIGURE 9. Local load controller.

inner current controller. The effect of the unbalanced current flowing in the neutral is compensated with a PR controller in 0-axis of $\alpha\beta 0$ -reference in the inner current controller. The block diagram of the inner current controller is shown in Figure 8.

D. LOCAL LOAD CONTROLLER

The test microgrid has been made more realistic by adding different rating local loads in each DG terminal in addition to the loads connected from the PCC. When local loads are connected in DGs' terminal, the virtual line voltage drops across the controller become unequal due to the additional local currents. Hence, the power-sharing, mostly reactive power being dependent on the voltages get disturbed severely. The effect of local loads is compensated with the help of a local load controller, which gives the additional virtual voltage drop seen across the controller due to the local loads. The local load virtual voltage drops are calculated using equations 17 & 18.

$$V_{vlocal1} = I_{1local} \times Z_{1v} \quad (17)$$

$$V_{vlocal2} = I_{2local} \times Z_2 \quad (18)$$

where Z_{1v} & Z_2 are the mainline impedances seen across their voltage controllers. For the DG having lower line impedance, it is equal to the sum of actual line impedance and the virtual impedance. For the other DG, it is equal to the actual line impedance. The block diagram of the local load controller is shown in Figure 9.

TABLE 1. Simulation parameters.

S.N.	Description of Parameters	Value
1	V_{dc}	800 V
2	PWM switching frequency	18000 Hz
3	Filter L and C	1.46 mH and 30.8 μ F
4	Line impedance L_1 and L_2	$0.2 + j0.6$ and $0.4 + j1.2$
5	Neutral line impedance L_{n1} and L_{n2}	$0.2 + j0.6$ and $0.4 + j1.2$
6	Droop coefficients m, m_p and n	0.001, 0.001 and 0.0012
7	Virtual impedance R_v , X_v and Z_{0v}	0.2, 0.6 and 1.44
8	Voltage controller gains K_p , K_i	0.35 and 25
9	Current controller gains K_p , K_i	0.7 and 500

TABLE 2. Details of loads used in case-1.

S.N.	Description of Parameters	Value	Remarks
1	PCC balanced load, P(w)+iQ(var)	6000+j2400	Always connected
2	PCC unbalanced load, P(w)+iQ(var)	Phase A: 2000+j800 Phase B: 4000+j1600 Phase C: 6000+j2400	Connected to PCC from 1s to 2s of the simulation.

V. TEST RESULTS AND DISCUSSION

This section will be sub-divided into two sub-section: (A) Simulation environment, and (B) Laboratory based environment.

A. SIMULATION ENVIRONMENT

Firstly, the proposed concept of the controller is studied within a simulation environment by using a powerful simulation tool called MATLAB/ Simulink software. To demonstrate the effectiveness of the proposed control scheme under unbalanced and local loads, two cases are considered in this study. The considered cases are described in detail and presented in sub-sections. While simulation, some assumptions had been made regarding the parameters, which are listed in Table 1.

1) CASE-1: UNBALANCED LOAD

In this case, the balanced as well as the unbalanced loads are supplied from PCC. The performance of the proposed control scheme is analyzed by measuring the DG terminal voltages, DG currents, active and reactive power-sharing, negative sequence reactive power, and voltage unbalanced factor (VUF). For the sake of simplicity, the local loads are not considered in this case. The load parameters used in this case are summarized in Table 2.

The simulation of the test system is run for three seconds. Initially, the test system supplies the balanced loads only, and then the unbalanced load is connected to the system from one second (1s) to 2s. The performance observed with the conventional droop control method is presented in Figure 10.

The load starts drawing an unbalance current when the unbalanced load is connected to the PCC at 1s. It causes the the DGs' terminal voltages to become unbalanced due to unbalanced drop in the DGs' internal impedance, as shown in Figure 10a. When the unbalanced portion of the voltages

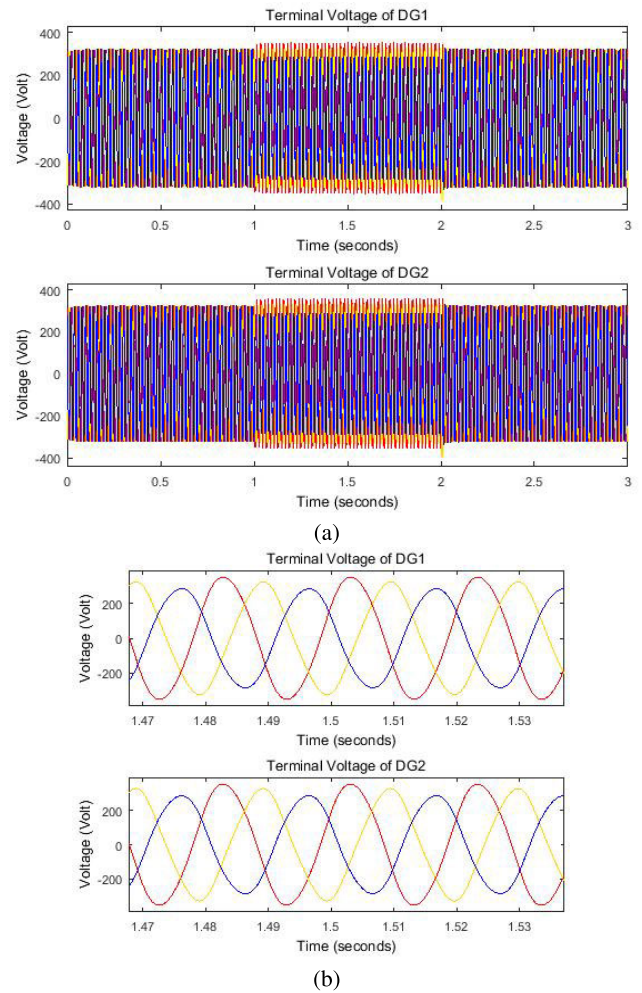


FIGURE 10. DG terminal voltages with conventional droop control.

are zoomed, it can be seen that phase with smaller load has small reduction in the voltage and the phase with larger load has voltage reduced the most, as shown in Figure 10b. This happens because of the large voltage drop in the DG internal impedance. The VUFs of the DGs' terminal voltages reached to 4% with conventional droop control under an unbalanced load, which can be seen in Figure 11. Furthermore, the negative sequence reactive power is not shared accurately with the conventional droop and virtual impedance loop. The unequalized distribution of the negative sequence reactive power is shown in Figure 12. The DG_2 (having higher line impedance) has shared more negative sequence reactive power than the other.

When the proposed control method is applied to the considered test system, the performance seems to be improved. The DGs' terminal voltages are now balanced even when the unbalanced load at the PCC draws an unequal current as presented in Figure 13.

During these processes, the current waveforms are in unbalanced condition as shown in Figure 14. However, the

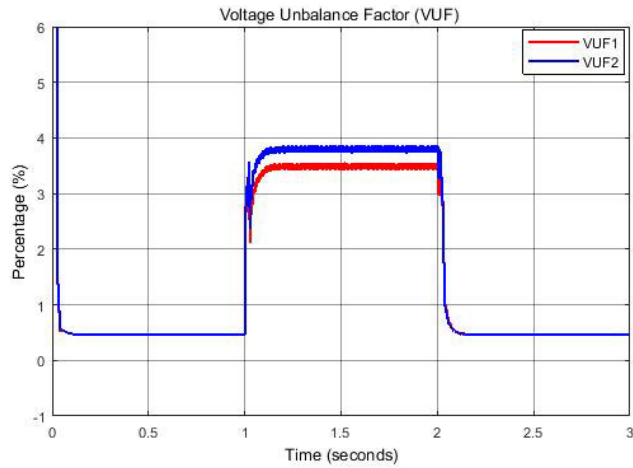
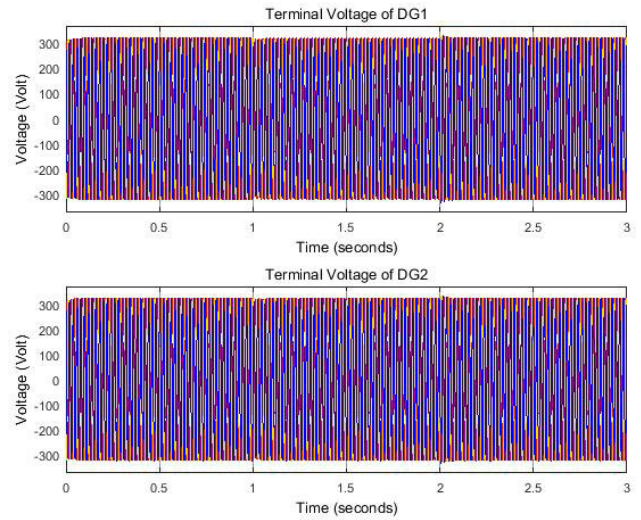
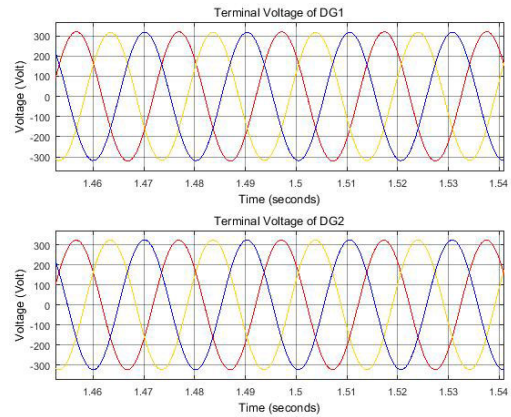


FIGURE 11. VUFs with conventional droop control.



(a)



(b)

FIGURE 13. DG terminal Voltages with the proposed control scheme.

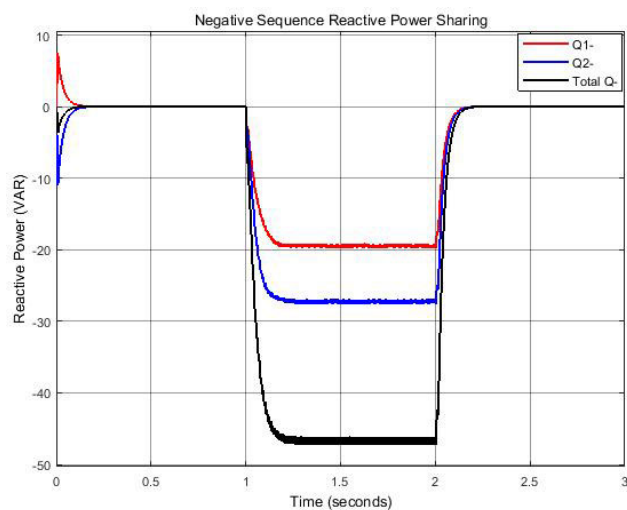


FIGURE 12. Negative sequence reactive power with conventional VI loop.

DGs' currents are found to be correlated with the load shared by the DGs.

One of the important observations for the proposed method is that the VUFs of the DGs' terminal voltages are reduced from 4% to 1% while supplying the unbalanced load. The dynamic characteristics of the VUFs for both of the DGs can be seen in Figure 15. In addition, the negative sequence reactive power in the system is significantly reduced while applying the positive sequence power components within the droop controller. The nature of the negative sequence reactive powers is shown in Figure 16.

When a balanced or unbalanced load is added to the system, both DGs have supplied an equal amount of active and reactive power. Similarly, whenever an active or reactive load is removed from the system, the active or reactive power shared by each DG is decreased by half of the load removed. This processes can be seen in Figures 17 and 18. From this performance it can be said that the power-sharing is improved

with the proposed control scheme as the influence of negative sequence components is compensated significantly.

The conventional virtual impedance loop based on α & β axes ignores the unbalanced current flowing in the neutral so that the DG neutrals are unequally sharing the unbalance. In this paper conventional virtual impedance loop has been modified incorporating 0-axis so that the DG neutral currents are also made equal whenever the DGs are sharing equal unbalanced power as shown in Figure 19.

Similarly, the frequency response of the conventional controller is shown in Figure 20. The system frequency is decreased whenever the load is added to the system and increased whenever the load is removed from the system. Here in this case, no system is applied to restore the system frequency and the system stability. It is just presented to determine the maximum deviation of the frequency in the system if load is changed accidentally. Although no restoring system is implemented, the system frequency has remained within the standard frequency deviation limit of 2.5%. On the other side, the system frequency can be maintained within a

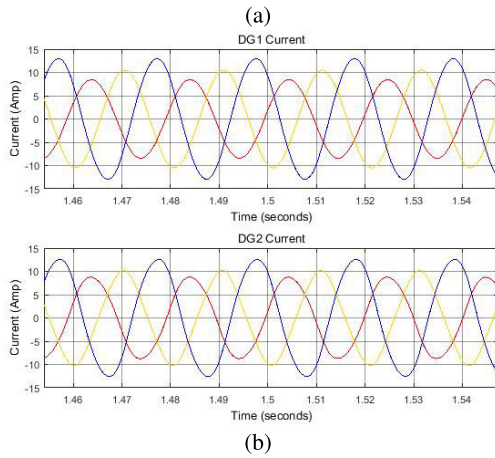
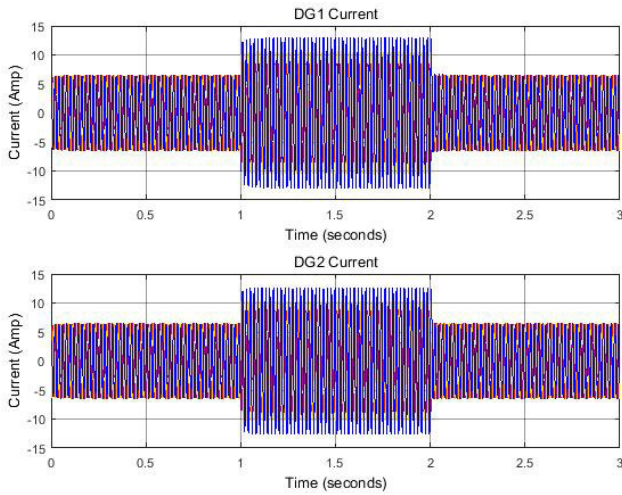


FIGURE 14. DG currents with the proposed control scheme.

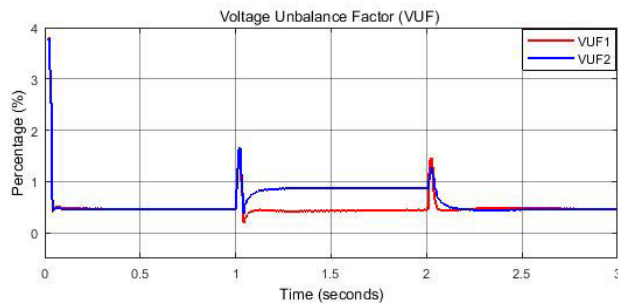


FIGURE 15. VUF With the proposed control scheme.

permissible limit despite any active load change by choosing a suitable P/F-droop coefficient.

2) CASE-2: PRESENCE OF LOCAL LOADS

Similarly, in second case, the unequal local loads are applied to the local lines with a certain line impedance, and connected to the DGs’ terminals. However, the considered DGs are identical with equal droop coefficients. The detail values of the considered parameters are given in Table 3.

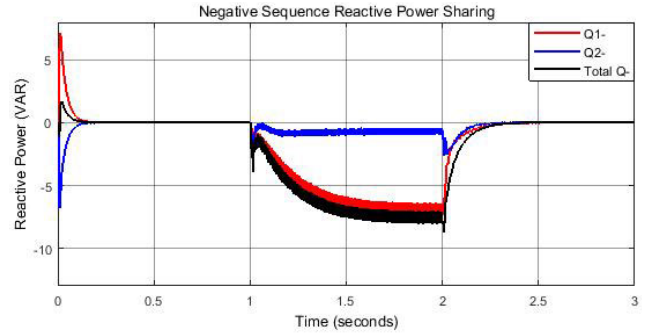


FIGURE 16. Negative sequence reactive power with the proposed control scheme.

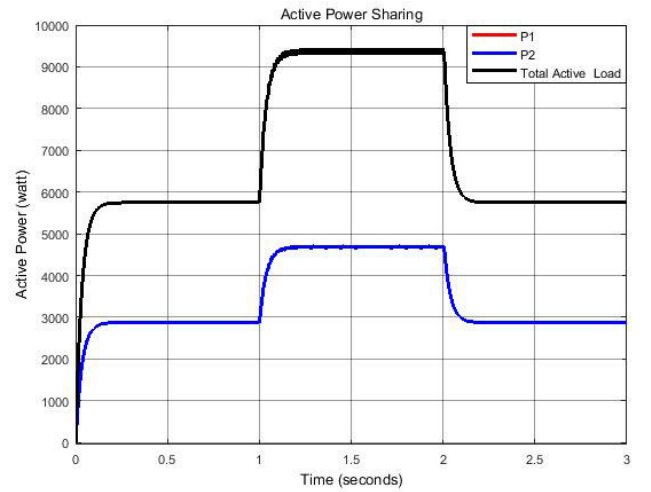


FIGURE 17. Active power-sharing.

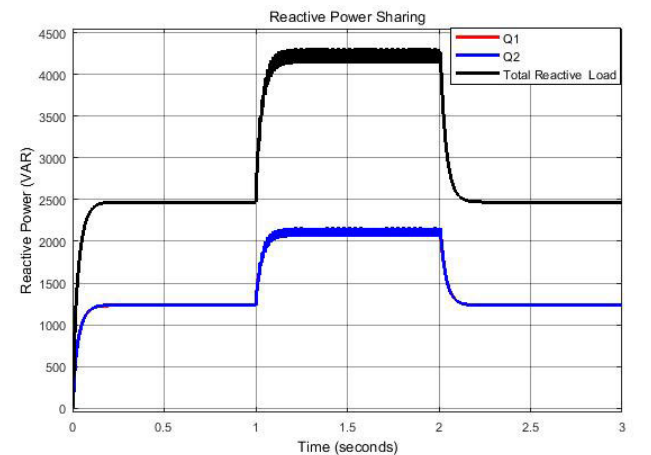
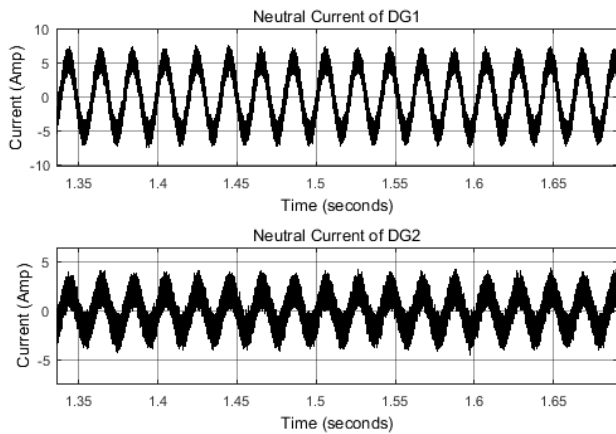
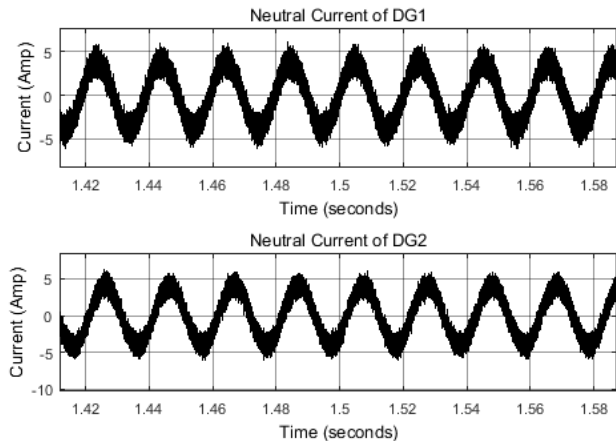


FIGURE 18. Reactive power-sharing.

The local lines impedances are, $Z_{1local} = 0.3 + j0.5$ & $Z_{2local} = 0.6 + j1$. The values for local load controllers used in both DGs are $R_v + jX_v = 0.4 + j1.2$. Initially, the simulation of the test system is run with $PCC load_1$ and $local load_1$.



(a) With conventional VI loop.



(b) With the proposed VI loop

FIGURE 19. DG neutral currents.

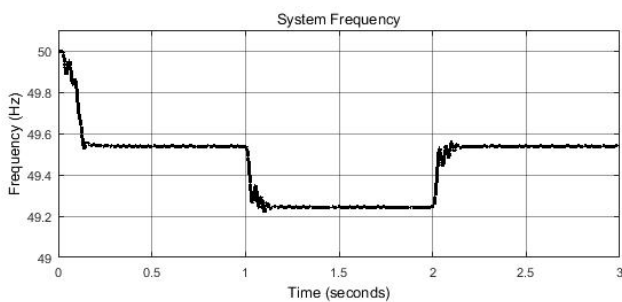


FIGURE 20. System frequency.

TABLE 3. Details of loads used in Case-2.

S.N	Description of Loads	Value	Remarks
1	PCC Load ₁	$6000 + j2400$	Always Connected
2	PCC Load ₂	$6000 + j2400$	1.5s to 2s
3	DG ₁ LocalLoad ₁	$2000 + j800$	Always Connected
4	DG ₁ LocalLoad ₂	$2000 + j800$	0.5s to 3s
5	DG ₂ LocalLoad ₁	$4000 + j1600$	Always Connected
6	DG ₂ LocalLoad ₂	$4000 + j1600$	1s to 2.5s

Then PCC load and local loads are varied in the time interval as described in Table 3.

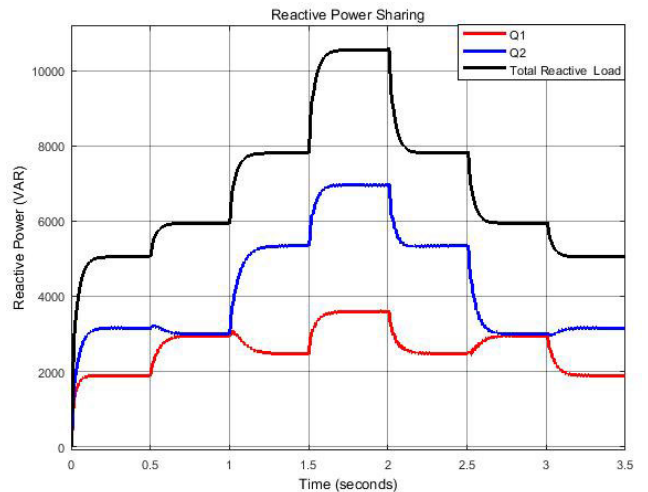


FIGURE 21. Reactive power-sharing without local load controller.

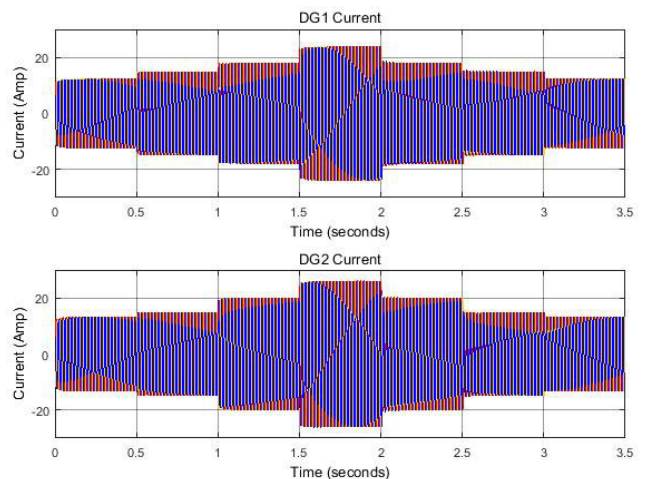


FIGURE 22. DG currents without local load controller.

The distribution of reactive power-sharing without the local load controlled is shown in Figure 21. When the local reactive load of DG_1 is increased at 0.5s, it is supplied by the DG_1 only. Similarly, when the local reactive load of DG_2 is increased at 1s, it is supplied by the DG_2 only. However, the PCC reactive load is shared equally when it is added at 1.5s. Similar cases when the reactive local loads of each DG are decreased. The reactive power-sharing with local loads is affected by local line currents. Thus, when the DG takes its entire local load itself in absence of the local load controller, its local line current increases, and the reactive power-sharing of other the DG gets decreased slightly due to further increase in its local line current. This results in an unequal loading of DGs as shown in Figure 22.

With the help of the proposed local load controller, the effect of local loads on the reactive power-sharing is compensated and the reactive power-sharing of each DG is made equal even when the reactive load is changed in each DG terminal as shown in Figure 23. Thus, the current loading of

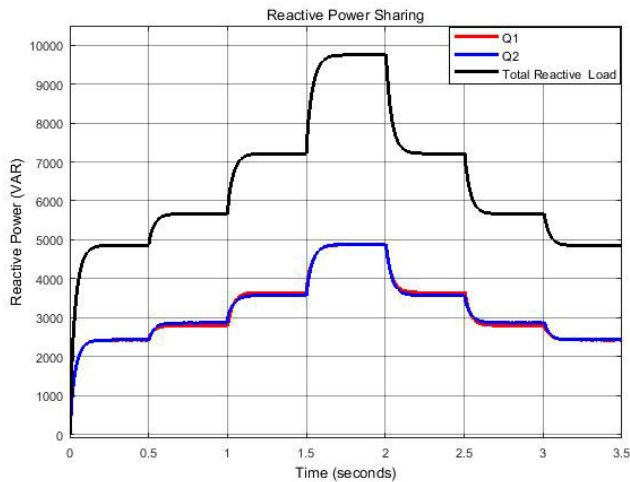


FIGURE 23. Reactive power-sharing with local load controller.

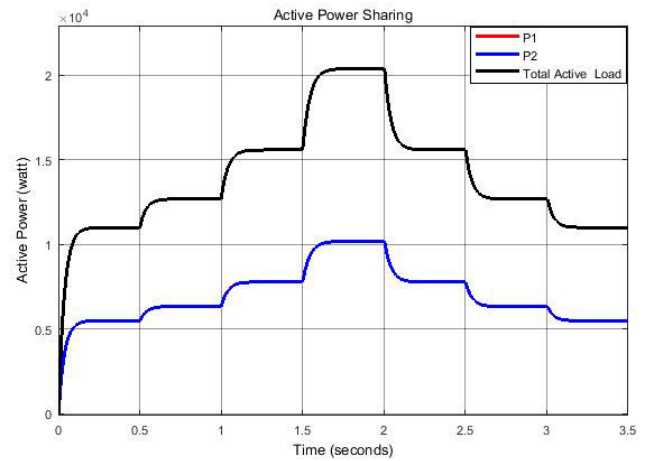


FIGURE 25. Active power-sharing with local load controller.

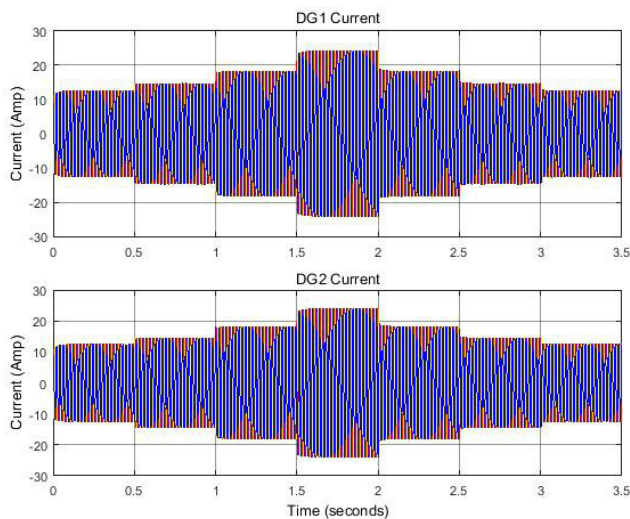


FIGURE 24. DG currents with local load controller.

DGs is identical as shown in Figure 24. Also, whenever the active load is added or removed to/from the system (i.e. either at PCC or DG terminal) the change is equally shared by both DGs as shown in Figure 25.

B. LABORATORY BASED ENVIRONMENT

After obtaining the simulation results, experimental validation work is done in a laboratory-based environment of Opal-RT. An Opal-RT-4510 Rapid Control Prototyping System is used for real-time simulation. The system is a part of a large platform called the Smart Power Platform of the IREENA Laboratory. The Opal-RT-4510 testing system comprises target nodes, oscilloscope, host PC, real-time and Ethernet communication links, and input and output boards. A picture of the lab setup can be seen in Figure 26. The power circuit, controller, and load parameters used for the experiment are similar to those used in previous simulation work as described in Tables 1 and 2. The validation work is done for both

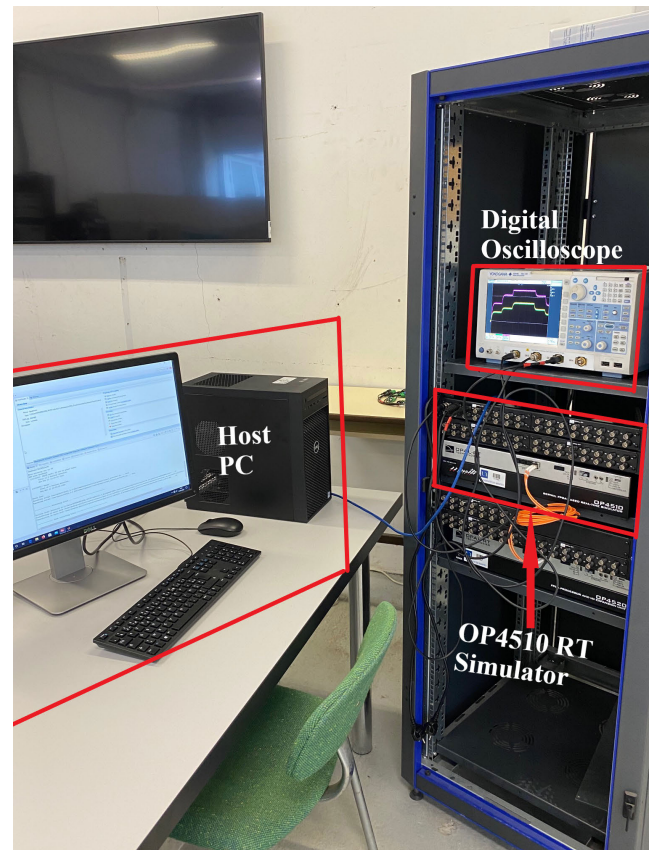


FIGURE 26. Experimental setup for real-time simulation.

considered cases. It is observed that the experimental results obtained are found to be similar to those obtained with simulation previously. Some of the major findings are described here. The system runs with the balanced loads initially and unbalanced loads are switched into the system at 1s. The unbalanced load at PCC draws an unbalanced current from the DGs, which causes an unbalanced voltage drop in the internal impedances of DGs. This makes the DGs' terminal

TABLE 4. Summary of the proposed control strategy.

S.N.	Issue	Proposed Solution	Key Benefits
1	Development of a three-phase four-wire system	NPC inverter are used to form the three-phase four-wire system by connecting the neutral point of the inverter to the load neutral.	i). Matured technology and being manufactured globally. ii). Low stresses on the switches in high-power applications. iii). No control difficulty iv). Low harmonics
2	Issues of conventional droop control method: Inherent drop, Poor transient response, and Trade-off between power-sharing and power quality.	i). Angle droop equation is used instead of frequency droop. ii). The conventional angle droop equation is modified by incorporating an integral term to improve the dynamic response of power-sharing.	i). Better regulation of system frequency in the steady state. ii). The used active power/angle droop equation acts as a proportional-derivative (PD) controller for frequency and reduces overshoots. iii). Improved dynamic response of power-sharing.
3	Power-sharing under unbalanced loads condition.	i). Improved virtual impedance incorporating zero axis impedance. ii). To enable an accurate sharing of effective powers under unbalanced loads, only positive sequence components of powers are used in the droop equations to generate a symmetrical voltage reference for inner controllers.	i). Zero sequence current (neutral current) can be controlled and compensated. ii). The influence of zero sequence components and negative sequence components in power-sharing is reduced. iii). An accurate sharing of effective powers.
4	Maintenance of system parameters (Voltage and Frequency).	i). Improved angle droop equation for better frequency regulation in transient and steady state. ii). Improved inner current and voltage controller incorporating PR controllers in all three axes of stationary $\alpha\beta 0$ reference frame for better tracking of symmetrical sinusoidal reference obtained from droop controller.	i). System parameters are strictly maintained within the prescribed limits against load disturbances. ii). Benefits from the use of PR controllers: Better tracking of sinusoidal reference with zero tracking error, avoids a number of transformations, and is suitable for the unbalanced and harmonic loads situation.
5	Local loads at DG terminals	A local load controller has been proposed to control the reactive power-sharing when local loads of different ratings are switched at the DG terminals.	i). Reactive power-sharing control is possible. ii). Overloading of DGs can be avoided. iii). Line loss can be minimized.

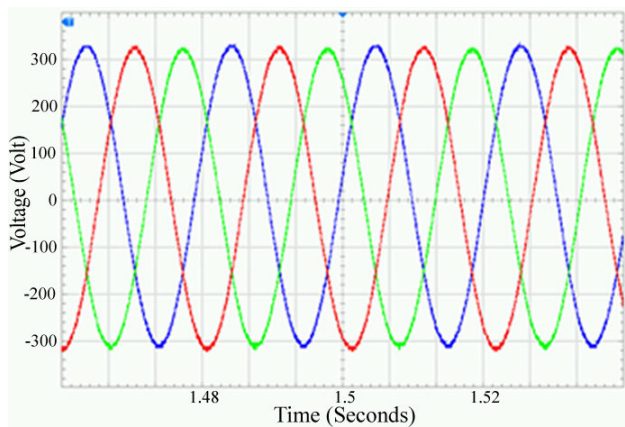


FIGURE 27. DG terminal voltage of DG1.

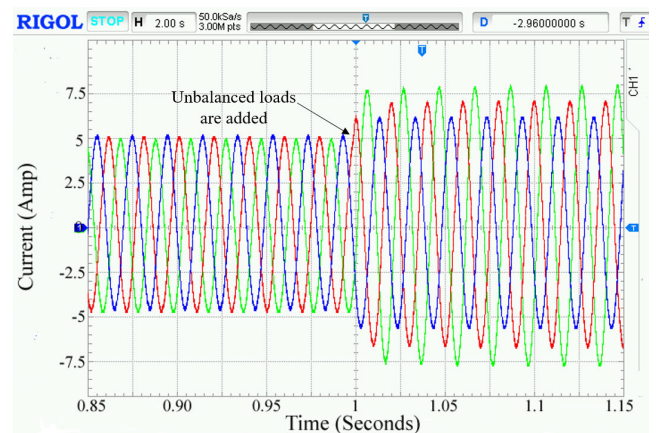


FIGURE 28. DG1 current.

voltages unbalanced. With the proposed control scheme, the DGs’ terminal voltages are found to be balanced throughout the time considered despite the load change. The measurement of the VUFs of the DGs’ terminal voltages quantifies the unbalance. The VUFs of the DGs’ terminal voltages are reduced from almost 4% to less than 1%, which is an acceptable value according to the current international standards. The nature of the terminal voltage and DG current are shown in Figure 27 and 28 respectively.

Table 4 summarises the performance of the proposed control scheme as compared to the conventional droop control

method and other competing alternatives in dealing with the following operational issues.

For the second case, the details of local and PCC loads are similar to those described in Table 3. Both active and reactive loads are varied to observe the controller performance. The system starts with certain loads at DGs’ terminals and PCC. At 0.5 seconds, active and reactive local loads are added at both DG’s terminals. Similarly, active and reactive loads are connected to the PCC at 1s. The active load has been shared equally whenever the load is either added to DGs’ terminals or at the PCC as shown in Figure 29.

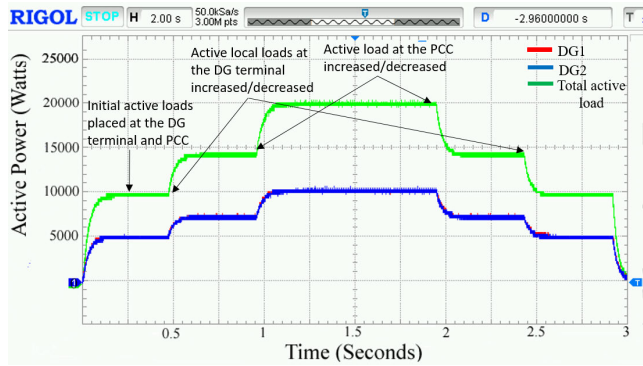


FIGURE 29. Active power-sharing.

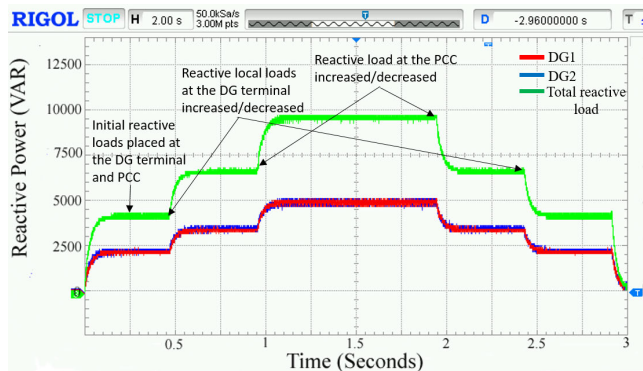


FIGURE 30. Reactive power-sharing.

However, the local reactive load isn't shared equally by the DGs without the proposed controller. But with the application of the proposed local load controller, it is made equal as shown in Figure 30.

VI. CONCLUSION

A control scheme for the three-level NPC inverters-based three-phase four-wire microgrid with balanced and unbalanced loads is proposed in this paper. With this control scheme, the system parameters (voltage and frequency) are closely regulated within their standard permissible limits against several balanced and unbalanced load disturbances. Application of proposed control strategy has reduced the VUFs of DGs' terminal voltages from 4% to less than 1% while supplying unbalanced loads. The observed reduction in the negative sequence reactive power after the use of the proposed control strategy also ascertains the compensation of unbalance. The proposed virtual impedance has performed two roles: one is impedance matching for accurate reactive power-sharing, and another is neutral current control. Thus, equal currents in the DGs' neutrals have been achieved with the proposed virtual impedance loop while sharing the unbalanced loads. Furthermore, the proposed droop controller acting only on the positive sequence components of powers reduces the impact of other sequence components in power-sharing. Moreover, different rating local loads are considered in each DG terminal to make the test microgrid

more realistic. The presence of local loads disturbs the power-sharing mostly reactive as the voltage drop in the DGs differs with the unequal local line currents. Consequently, a local load controller is proposed to compensate the effects of local loads in the voltage controller and improve the reactive power-sharing. Hence, all in all, the proposed control strategy contributes to improved power-sharing under unbalanced loads. The claimed performances of the proposed control scheme are also validated through an Opal-RT laboratory environment.

REFERENCES

- [1] P. Piagi and R. H. Lasseter, "Autonomous control of microgrids," in *Proc. IEEE Power Eng. Soc. Gen. Meeting*, Jun. 2006, p. 8.
- [2] R. Lasseter, "MicroGrids," in *Proc. IEEE Power Eng. Soc. Winter Meeting*, vol. 1, Jan. 2002, pp. 305–308.
- [3] X. Wang, J. M. Guerrero, F. Blaabjerg, and Z. Chen, "A review of power electronics based microgrids," *Int. J. Power Electron.*, vol. 12, no. 1, pp. 181–192, 2012.
- [4] Z. Zeng and W. Shao, "Reconnection of micro-grid from islanded mode to grid-connected mode used sliding Goertzel transform based filter," *IET Renew. Power Gener.*, vol. 11, no. 7, pp. 1041–1048, Jun. 2017.
- [5] O. Palizban and K. Kauhaniemi, "Microgrid control principles in island mode operation," in *Proc. IEEE Grenoble Conf.*, Jun. 2013, pp. 1–6.
- [6] F. M. Ahmed, "Estimated droop control for parallel connected voltage source inverters: Stability enhancement," M.S. thesis, Dept. Health, Sci. Technol., Karlstad Univ., Karlstad, Sweden, 2013.
- [7] A. Raghmi, "A novel Thevenin-based voltage droop control improving reactive power sharing with structures to identify Thevenin parameters," Ph.D. dissertation, School Elect. Eng. Comput. Sci., Queensland Univ. Technol., Brisbane, QLD, Australia, 2019.
- [8] J. He and Y. W. Li, "Analysis, design, and implementation of virtual impedance for power electronics interfaced distributed generation," *IEEE Trans. Ind. Appl.*, vol. 47, no. 6, pp. 2525–2538, Nov. 2011.
- [9] S. Y. Altaf, X. Yan, and X. Liu, "A power sharing method for inverters in microgrid based on the virtual power and virtual impedance control," in *Proc. 11th IEEE Int. Conf. Compat., Power Electron. Power Eng. (CPE-POWERENG)*, Apr. 2017, pp. 151–156.
- [10] J. M. Guerrero, L. Garcia de Vicuna, J. Matas, M. Castilla, and J. Miret, "Output impedance design of parallel-connected UPS inverters with wireless load-sharing control," *IEEE Trans. Ind. Electron.*, vol. 52, no. 4, pp. 1126–1135, Aug. 2005.
- [11] J. M. Guerrero, N. Berbel, L. Garcia de Vicuna, J. Matas, J. Miret, and M. Castilla, "Droop control method for the parallel operation of online uninterruptible power systems using resistive output impedance," in *Proc. 21st Annu. IEEE Appl. Power Electron. Conf. Expo. (APEC)*, Mar. 2006, p. 7.
- [12] Y. A.-R. I. Mohamed and E. El-Saadany, "Adaptive decentralized droop controller to preserve power sharing stability of paralleled inverters in distributed generation microgrids," *IEEE Trans. Power Electron.*, vol. 23, no. 6, pp. 2806–2816, Nov. 2008.
- [13] J. M. Guerrero, J. C. Vasquez, J. Matas, L. G. de Vicuna, and M. Castilla, "Hierarchical control of droop-controlled AC and DC microgrids—a general approach toward standardization," *IEEE Trans. Ind. Electron.*, vol. 58, no. 1, pp. 158–172, Jan. 2011.
- [14] M. Savaghebi, A. Jalilian, J. C. Vasquez, and J. M. Guerrero, "Autonomous voltage unbalance compensation in an islanded droop-controlled microgrid," *IEEE Trans. Ind. Electron.*, vol. 60, no. 4, pp. 1390–1402, Apr. 2013.
- [15] B. Ren, X. Sun, S. Chen, and H. Liu, "A compensation control scheme of voltage unbalance using a combined three-phase inverter in an islanded microgrid," *Energies*, vol. 11, no. 9, p. 2486, Sep. 2018.
- [16] Z. Hanzelka and Y. Varetzky, "Negative-sequence active power stream as an index of unbalance source," in *Proc. 11th Int. Conf. Electr. Power Quality Utilisation*, Oct. 2011, pp. 1–4.
- [17] Y. Jia, D. Li, and Z. Chen, "Unbalanced power sharing for islanded droop-controlled microgrids," *J. Power Electron.*, vol. 19, no. 1, pp. 234–243, 2019.
- [18] M. Hamzeh, H. Karimi, H. Mokhtari, and J. Mahseredjian, "Control of a microgrid with unbalanced loads using virtual negative-sequence impedance loop," in *Proc. 5th Annu. Int. Power Electron., Drive Syst. Technol. Conf. (PEDSTC)*, Feb. 2014, pp. 78–83.

[19] A. S. Vijay, S. Doolla, and M. Chandorkar, "Varying negative sequence virtual impedance adaptively for enhanced unbalanced power sharing among DGs in islanded AC microgrids," *IEEE Trans. Energy Convers.*, vol. 36, no. 4, pp. 3271–3281, Dec. 2021.

[20] H. Nian, Y. Liao, M. Li, D. Sun, Y. Xu, and B. Hu, "Impedance modeling and stability analysis of three-phase four-leg grid-connected inverter considering zero-sequence," *IEEE Access*, vol. 9, pp. 83676–83687, 2021.

[21] F. Najafi, M. Hamzeh, and M. Fripp, "Unbalanced current sharing control in islanded low voltage microgrids," *Energies*, vol. 11, no. 10, p. 2776, Oct. 2018.

[22] Q. Liu, Y. Tao, X. Liu, Y. Deng, and X. He, "Voltage unbalance and harmonics compensation for islanded microgrid inverters," *IET Trans. Power Electron.*, vol. 7, no. 5, pp. 1055–1063, May 2014.

[23] B. Zhang, X. Han, C. Ren, D. Zhang, L. Wang, and T. Song, "Circulating current suppression method with adaptive virtual impedance for multi-bidirectional power converters under unbalanced conditions," *CSEE J. Power Energy Syst.*, vol. 9, no. 1, pp. 77–87, Jan. 2023.

[24] H. Liu, J. Zhou, W. Wang, and D. Xu, "Droop control scheme of a three-phase inverter for grid voltage unbalance compensation," *J. Power Electron.*, vol. 18, no. 4, pp. 1245–1254, 2018.

[25] R. Aboelsaud, A. Ibrahim, and A. Garganev, "Review of three-phase inverters control for unbalanced load compensation," *Int. J. Power Electron. Drive Syst.*, vol. 10, no. 1, p. 242, Mar. 2019.

[26] M. R. Miveh, M. F. Rahmat, A. A. Ghadimi, and M. W. Mustafa, "Control techniques for three-phase four-leg voltage source inverters in autonomous microgrids: A review," *Renew. Sustain. Energy Rev.*, vol. 54, pp. 1592–1610, Feb. 2016.

[27] P. Yang, W. Ming, J. Liang, and J. Wu, "A four-leg buck inverter for three-phase four-wire systems with the function of reducing DC-bus ripples," in *Proc. 45th Annu. Conf. IEEE Ind. Electron. Soc. (IECON)*, Oct. 2019, pp. 1508–1513.

[28] J. Liang, T. C. Green, C. Feng, and G. Weiss, "Increasing voltage utilization in split-link, four-wire inverters," *IEEE Trans. Power Electron.*, vol. 24, no. 6, pp. 1562–1569, Jun. 2009.

[29] L. Wang, D. Zhang, Y. Wang, B. Wu, and H. S. Athab, "Power and voltage balance control of a novel three-phase solid-state transformer using multilevel cascaded H-bridge inverters for microgrid applications," *IEEE Trans. Power Electron.*, vol. 31, no. 4, pp. 3289–3301, Apr. 2016.

[30] M. Barghi Latran and A. Teke, "Investigation of multilevel multifunctional grid connected inverter topologies and control strategies used in photovoltaic systems," *Renew. Sustain. Energy Rev.*, vol. 42, pp. 361–376, Feb. 2015.

[31] C. Wang, Z. Li, X. Si, and H. Xin, "Control of neutral-point voltage in three-phase four-wire three-level NPC inverter based on the disassembly of zero level," *CPSS Trans. Power Electron. Appl.*, vol. 3, no. 3, pp. 213–222, Sep. 2018.

[32] Y. Sun, Y. Liu, M. Su, H. Han, X. Li, and X. Li, "Topology and control of a split-capacitor four-wire current source inverter with leakage current suppression capability," *IEEE Trans. Power Electron.*, vol. 33, no. 12, pp. 10803–10814, Dec. 2018.

[33] S.-P. Kim, S.-G. Song, S.-J. Park, and F.-S. Kang, "Imbalance compensation of the grid current using effective and reactive power for split DC-link capacitor 3-leg inverter," *IEEE Access*, vol. 9, pp. 81189–81201, 2021.

[34] N.-Y. Dai, M.-C. Wong, and Y.-D. Han, "Application of a three-level NPC inverter as a three-phase four-wire power quality compensator by generalized 3DSVM," *IEEE Trans. Power Electron.*, vol. 21, no. 2, pp. 440–449, Mar. 2006.

[35] B. Sharma, A. Shrestha, Y. Terriche, A. Lashab, and J. M. Guerrero, "Sharing sequence components of reactive power in a three-phase four-wire islanded microgrid," *Electr. Power Syst. Res.*, vol. 213, Dec. 2022, Art. no. 108675. [Online]. Available: <https://www.sciencedirect.com/science/article/pii/S037877962200743X>

[36] A. S. Pabbewar and M. Kowsalya, "Three level neutral point clamped inverter using space vector modulation with proportional resonant controller," *Energy Proc.*, vol. 103, pp. 286–291, Dec. 2016.

[37] M. Hojabri, M. Hojabri, and A. Toudeshki, "Passive damping filter design and application for three-phase PV grid-connected inverter," *Int. J. Elect., Electron. Data Commun.*, vol. 3, no. 6, pp. 50–56, 2015.

[38] R. N. Beres, X. Wang, M. Liserre, F. Blaabjerg, and C. L. Bak, "A review of passive power filters for three-phase grid-connected voltage-source converters," *IEEE Trans. J. Emerg. Sel. Topics Power Electron.*, vol. 4, no. 1, pp. 54–69, Mar. 2016.

[39] J. M. Guerrero, J. Matas, L. García de Vicuña, M. Castilla, and J. Miret, "Wireless-control strategy for parallel operation of distributed-generation inverters," *IEEE Trans. Ind. Electron.*, vol. 53, no. 5, pp. 1461–1470, Oct. 2006.

[40] P. Rodriguez, A. V. Timbus, R. Teodorescu, M. Liserre, and F. Blaabjerg, "Flexible active power control of distributed power generation systems during grid faults," *IEEE Trans. Ind. Electron.*, vol. 54, no. 5, pp. 2583–2592, Oct. 2007.

[41] J. L. Afonso, M. J. S. Freitas, and J. S. Martins, "P-q theory power components calculations," in *Proc. IEEE Int. Symp. Ind. Electron.*, vol. 1, Jun. 2003, pp. 385–390.

[42] N. A. Ninad and L. A. C. Lopes, "Per-phase vector (dq) controlled three-phase grid-forming inverter for stand-alone systems," in *Proc. IEEE Int. Symp. Ind. Electron.*, Jun. 2011, pp. 1626–1631.



BINOD SHARMA received the bachelor's degree in electrical engineering and the master's degree in electrical engineering in distributed generation from IOE, Tribhuvan University (TU), Pashchimanchal Campus, Pokhara, Nepal, in 2016 and 2020, respectively. He has worked as an Assistant Lecturer for two years with the Kathmandu Institute of Technology and IOE, TU, Pashchimanchal Campus. For the last four and half years, he has been working with Nepal Electricity Authority, the government-owned leading power utility of Nepal. He is currently actively involved in awareness programs and welfare activities related to energy, electricity, and electrical engineering. He is also working as the Executive Secretary of the Electrical Engineer's Welfare Association, Nepal, a non-profit organization established for the welfare of electrical engineers of Nepal. He also writes informative articles for public awareness in the field of electrical safety and economical use of electricity, renewable energy sources in national-level newspapers, and magazines. He is also a learner and beginner as a researcher with few peer-reviewed publications in microgrid, distributed generation, energy, and related research fields.



PRABHAT KUMAR PANKAJ received the bachelor's degree in electrical engineering and the master's degree in power system engineering from IOE, Tribhuvan University (TU), Pulchowk Engineering Campus, Nepal, in 2010 and 2014, respectively. He has 12 years in power sector i.e., worked across various academic institutions, such as an Assistant Lecturer along with the responsibility of Head of the Department of Electronics and Computer Engineering, Janakpur Engineering College (JEC), TU, from 2011 to 2013, where he was a Lecturer along with the responsibility of Head of the Department of Electrical Engineering, Advanced College of Engineering & Management (ACEM), from 2013 to 2015, and joined NEA, in 2015. He is currently an Engineer with the System Operation Department, Nepal Electricity Authority of having around seven years of experience in energy and power management of integrated power system of Nepal. He has involved in real-time operation of power system of Nepal for four years as a real-time system operator and management of energy, management of SCADA system, and dealing with import power. His key experience includes power system analysis, modeling, reliability evaluation, forecasting, mathematical optimization, and day ahead market. He was also a Key Member amongst Reliability Evaluation Committee. He was also appreciated through "Excellent Work Appreciation Letter" and the prestigious Award of NEA, in 2022. He is uninterruptedly active in field of research through his supervision for master's thesis in microgrid, distributed generation, energy, stability, and reliability and related research fields.



YACINE TERRICHE received the B.S. degree in electrical engineering from the University of Science and Technology, Constantine, Algeria, in 2011, the M.S. degree in electrical engineering from the University of Constantine 1, Constantine, Algeria, and the Ph.D. degree in electrical engineering from Aalborg University, Aalborg, Denmark, in 2020. During his Ph.D. degree, he was worked as a Research Assistant with the Kaohsiung University of Science of Technology, Kaohsiung, Taiwan, from December 2019 to September 2020. From November 2020 to November 2021, he was worked as a Research Assistant with AAU Energy, Aalborg University, where he is currently a Postdoctoral Researcher with AAU Energy. His research interests include power electronics modeling and control, signal processing, power quality issues, microgrids, cyber security, active and passive power filters, static VAR compensators, and maritime microgrids.



ABDELHAKIM SAIM was born in Batna, Algeria, in 1990. He received the B.S. and M.S. degrees in electronics and control engineering from Blida University, Blida, Algeria, in 2010 and 2012, respectively, and the Ph.D. degree in control engineering from Tizi-Ouzou University, Tizi Ouzou, Algeria, in 2017. He has been an Associate Professor in control engineering with the Department of Control and Instrumentation, University of Sciences and Technology Houari Boumediene, Algiers, Algeria. Since 2022, he has been an Associate Professor with the IREENA Laboratory and the Electrical Engineering Department, Nantes University. His current research interests include the power quality and stability of microgrids in stationary and onboard applications.



ASHISH SHRESTHA (Member, IEEE) received the bachelor's degree in electrical and electronics engineering from the School of Engineering, Pokhara University, Nepal, and the master's degree in planning and operation of energy system from the School of Engineering, Kathmandu University, Nepal. He is currently pursuing the Ph.D. degree with the Department of Electrical Engineering, Information Technology and Cybernetics, University of South-Eastern Norway, Porsgrunn Campus, Norway. He was an Erasmus Mundus candidate with the Department of Electrical Engineering, Frederick University, Cyprus, funded by European Union. Before his Ph.D. degree, he was worked as a Lecturer with the Department of Electrical and Electronics Engineering and a Researcher (the activity Leader), Center for Electric Power Engineering (CEPE), Kathmandu University, Nepal, for three and half years. He was also involved in the problem-based-learning project funded by Erasmus+ program of EU and was leading a project under the funding of the Ministry of Foreign Affairs (MFA), Norway, as the Project Co-Principal Investigator. He has published 44 peer-reviewed journal articles and international conference papers and was assigned as a reviewer for numerous international conferences and peer-reviewed journals from IEEE, Springer, Elsevier, and IET. His research interests include power system dynamics, distributed generation resources, planning, and operation of energy systems.



CHUN-LIEN SU (Senior Member, IEEE) received the Diploma degree in electrical engineering from the National Kaohsiung University of Science and Technology (NKUST), Taiwan, in 1992, and the M.S. and Ph.D. degrees in electrical engineering from National Sun Yat-sen University, Taiwan, in 1997 and 2001, respectively. In 2002 and 2006, he was an Assistant Professor and an Associate Professor with the Department of Marine Engineering, National Kaohsiung Marine University, Taiwan, respectively. From 2012 to 2017, he was a Full Professor and the Director of the Energy and Control Research Center. From August 2017 to January 2018, he was a Visiting Professor with the Department of Energy Technology, Aalborg University, Denmark. He was the Director of the Maritime Training Center, NKUST, from February 2018 to July 2020, where he has been a Professor with the Department of Electrical Engineering, since August 2020, and the Director of the Center for Electrical Power and Energy. His research interests include power systems analysis and computing, power quality, maritime microgrids, and offshore energy, recently specially focused on electrical infrastructure for offshore wind farms and maritime microgrids for electrical ships, vessels, ferries, and seaports. He received the Best Paper Prize of the Industrial and Commercial Power Systems Conference at IEEE-IAS, from 2012 to 2013, and the Best Paper Award of the IEEE International Conference on Smart Grid and Clean Energy Technologies, in 2018. He was a Guest Editor of the Special Issue on Next Generation Intelligent Maritime Grids of the IEEE TRANSACTIONS ON INDUSTRIAL INFORMATICS, in 2017, and the Special Issue on Power Quality and Protection in Renewable Energy Systems and Microgrids of *IET Renewable Power Generation*, in 2019.



JOSEP M. GUERRERO (Fellow, IEEE) received the B.S. degree in telecommunications engineering, the M.S. degree in electronics engineering, and the Ph.D. degree in power electronics from the Technical University of Catalonia, Barcelona, in 1997, 2000, and 2003, respectively. Since 2011, he has been a Full Professor with the Department of Energy Technology, Aalborg University, Denmark, where he is responsible for the Microgrid Research Program. He has been a Chair Professor with Shandong University, since 2014, a Distinguished Guest Professor with Hunan University, since 2015, a Visiting Professor Fellow with Aston University, U.K., since 2016, and a Guest Professor with the Nanjing University of Posts and Telecommunications. In 2019, he became a Villum Investigator. He has published more than 500 journal articles in the fields of microgrids and renewable energy systems, which are cited more than 30,000 times. His research interests include oriented to different microgrid aspects, including power electronics, distributed energy storage systems, hierarchical and cooperative control, energy management systems, smart metering, and the Internet of Things for AC/DC microgrid clusters and islanded minigrids, recently specially focused on maritime microgrids for electrical ships, vessels, ferries, and seaports. In 2015, he was elevated as a fellow of IEEE for his contributions on "Distributed power systems and microgrids." He received the Best Paper Award of the IEEE TRANSACTIONS ON ENERGY CONVERSION, from 2014 to 2015, the Best Paper Prize of IEEE-PES, in 2015, and the Best Paper Award of the *Journal of Power Electronics*, in 2016. For five consecutive years, from 2014 to 2018, he was awarded by Clarivate Analytics (former Thomson Reuters) as the Highly Cited Researcher. He is also an associate editor for a number of IEEE TRANSACTIONS.

...